Available online at www.sciencedirect.com

ScienceDirect

Energy Procedia 105 (2017) 1564 – 1569

Energy Procedia

The 8th International Conference on Applied Energy ICAE2016

Numerical assessment of an automotive derivative CHP fuel cell system

Andrea Luigi Facci[a,*], Gabriele Loreti[a], Stefano Ubertini[a], Frano Barbir[c], Thomas Chalkidis[d], Rolf-Peter Eßling[e], Thijs Peters[f], Efthalia Skoufa[g], Roberto Bove[b]

[a]*School of engineering, University of Tuscia, Italy*
[b]*General Electric Switzerland GmbH*
[c]*University of Split, Croatia.*
[d]*HELBIO S.A., Greece*
[e]*SINTEF Norway*
[f]*NuCellSys GmbH, Germany*[f]
[g]*Alstom Power UK*

Abstract

In this paper we model the performance of a PEM-based CHP system. Such a system represents the first layout under investigation within the AutoRe project, which aims at developing an automotive derivative CHP stationary system based on PEM fuel cells with an electrical power in the range 50 kW - 100 kW. The CHP system is fed with natural gas (NG). The model is developed in Aspen-plus with proprietary Fortran codes for the FC and the PSA. Two configurations are studied: with one and with two fuel cell stacks. The performance is presented in terms of electric and thermal power outputs and efficiencies.

Peer-review under responsibility of the scientific committee of the 8th International Conference on Applied Energy.

Keywords: CHP; Hydrogen; Fuel Cells; PEM

1. Introduction

In the last two decades, different fuel cell technologies have been developed and some have entered the market of distributed CHP systems. Most of the installations worldwide are micro-CHP systems with a nominal power lower than 5 kW [1-4]. Asia dominates this fuel cell market with more than 90,000 installations in Japan by 2013. North America follows, with more than 300 installations (about 100 are CHP systems), while, in Europe, the installations are slightly less than 1,000 [5-7]. The attributes such as low weight, quick response in power output and low design challenges and the results achieved, in terms of efficiency, reliability and durability, across a wide range of applications, including automotive, CHP systems, distributed back-up power and micro-applications in portable devices, have made PEM the most mature FC technology for rapid commercialization. At the end of 2012, PEMFC represented almost the 88% of the total fuel cell market with all the units sold with an electrical power below 5 kW [2]. SOFCs are still in a pre-commercial stage, with only few demonstration units available. Fuel cell energy systems in the power range 5-100 kW are mostly MCFCs, with less than 10 units in Europe and hundreds worldwide, although a market potential of thousands of installation per year. Only few data are available regarding the performance of these systems, although several fuel cell CHP systems are operating worldwide. Electrical efficiencies for micro-CHP systems declared by the manufacturers are all below 40%. CHP systems based on PEM fuel cells have been also extensively studied in the scientific literature, with several papers dealing with experimental analyses [8-10] and numerical modeling [11, 12] in the last decade, all characterized by an electrical power output well below 50 kW.

* Corresponding author. Tel.: +39 0761 357676.
E-mail address: andrea.facci@unitus.it.

Peer-review under responsibility of the scientific committee of the 8th International Conference on Applied Energy.
doi:10.1016/j.egypro.2017.03.495

Cost is the major obstacle to a massive production of PEM-based energy systems, despite a significant reduction in the last decade (more than 80% since 2002 and 35% since 2008). Cost estimates are at least an order of magnitude higher than the target of 500-1,000 $/kW [1-3, 7].

In this paper we numerically investigate the performance of a PEM based CHP system, which represents the first layout under investigation within the AutoRe project, funded under the Horizon 2020. This project aims at developing an automotive derivative CHP stationary system based on PEM fuel cells with an electrical power in the range 50 kW-100 kW. The cooperation among industries from different sectors (i.e. stationary power systems and automotive) should allow a significant reduction of capital costs compared to the state of the art by increasing the production volume and facilitating the technological transfer among different industries. Within the project, we will also develop and employ innovative solutions for reducing complexity and costs of balance of plant and reforming units, thus allowing for an even more cost-competitive system. The CHP system is fed with natural gas (NG), such that a fuel processor is required to convert NG into a hydrogen rich reformate. The developed numerical model will be utilized to estimate the performances of the baseline prototype for the AutoRe project, to support the experimental tests and to evaluate possible improvements and alternative configurations.

2. Description of the PEM based CHP concept

The baseline concept of the PEM based CHP plant that is modeled throughout this paper is represented in Fig. 1. It is composed by two main sections: the fuel processor and the fuel cell. The fuel processor transforms NG into H_2, whose purity can exceed 99.999%. The fuel cell is modeled according to real process data as provided by the manufacturers.

About 5% of the total amount of NG, together with tail gas from the PSA and oxidizing air, is directed to the combustor, which provides the energy necessary for the endothermic steam reforming (SR). The combustor is operated at ambient pressure and 790°C. The air is pre-heated exchanging energy with the combustion flue gas, through the heat exchanger HE-2. The majority of the NG is compressed to 12 bar and mixed with superheated steam at a temperature of 220°C. Such a mixture, before entering the Steam Reformer (SR), is heated in the heat exchanger HE-3 through the hot syngas exiting the SR. Then, in the SR, it is converted into a syngas primarily composed of H_2 and CO. The SR and the burner are integrated within the same component, following the concept of the Heat Integrated Wall Reactor (HIWAR) [14-15]. After the heat exchanger HE-3, the syngas is cooled down to 410°C and the CO concentration is reduced in a water gas shift reactor (WGSR). The thermal energy of the syngas at the WGSR outlet is transferred to the water necessary for the SR in the heat exchanger HE-5. The syngas temperature at the HE-5 outlet is 118°C, and is further reduced to 5°C through the heat exchangers HE-6 and HE-7. Syngas is finally purified through a Pressure Swing Adsorption (PSA). Impurities are adsorbed at high pressure and then are rejected reducing the system pressure (pressure swing). The unrecovered H_2 and separated impurities are burned in the combustor.

Liquid water is compressed to 12 bar through a dedicated pump, pre-heated and partially vaporized in HE-5. Vaporization and superheating are completed in HE-1, where the steam is heated by the hot burner exhaust gas. The ratio between the water and NG mass flow rates is fixed to 3.73. Under design conditions the reformer delivers pure hydrogen at a pressure of 11 bar and at a temperature of about 5°C. The hydrogen is then fed to the FC that produces electricity and thermal power as byproduct. The maximum continuous electrical power of the complete system is about 55 kW. Since the FC is operated at a temperature of 80°C, the co-generated heat is available at a temperature $T_{cog} < 80°C$, and can be utilized for domestic or civil applications, such as space heating or domestic hot water.

The CHP plant features an automotive derivative PEM FC designed and produced by NuCellSys. The production of a small series of the Mercedes-Benz B-Class powered by a PEM stack started in 2009. The reliability of the FC based powertrain was demonstrated at the fuel cell world drive in 2011 and by reaching 300.000 km with a single car in 2014. Such a system includes the FC and a control system that regulates hydrogen and oxygen flows according to the operating conditions. A coolant circuit ensures that the FC is kept at an operating temperature of 80°C, and provides the thermal energy for co-generation.

3. Numerical Model

The steady state modelling of the power plant described in section 2 is performed through a thermodynamic lumped parameter approach, except for the PSA and the FC that are simulated through black-box phenomenological models. Simulations are carried out in Aspen Plus [16] combined with proprietary Fortran models for the FC and the PSA. Our approach is consistent with other analyses available in literature, as those available in [10, 11]. The relevant performance parameters for the CHP plant in study are the gross electrical power, P_{el}, the thermal power, Q_{cog}, the electrical efficiency of the prime mover, $\eta_{FC} = P_{el}/(\dot{m}_{H2}\, H_i)$, the global electrical efficiency of the plant, $\eta_g = (P_{el} - W_{aux})/(\dot{m}_{CH4}\, H_i)$, and the first law or total efficiency, $\eta_t = (P_{el} - W_{aux} + Q_{cog})/(\dot{m}_{CH4}\, H_i)$. In the

previous relationships $\dot{m}_{H2}$ is the H_2 mass flow rate at the FC inlet, H_i is the NG lower heating value, $\dot{m}_{CH4}$ is the NG mass flow rate, W_{aux} is the power consumed by the auxiliaries, and Q_{cog} is the thermal energy production.

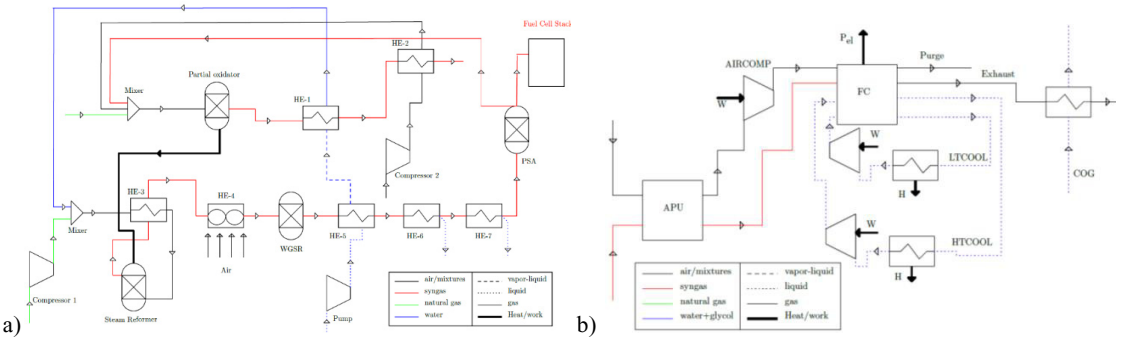

Fig. 1 - Schematic of the CHP plan concept modelled throughout the paper: a) energy system; b) fuel cell.

The relevant submodels of the fuel processor regards the following components: (i) the NG burner; (ii) the steam reforming reactor; (iii) the water gas shift reactor; (iv) the PSA; and (v) the heat exchangers. Both the burner and the steam reformer are modeled through an Aspen Plus module that minimizes the Gibbs free energy to determine the equilibrium composition, given the initial reactants composition and the reactor temperature [14]. The NG mass flow rate is determined by imposing a burner temperature of 790°C. The water gas shift reactor is modeled through a stoichiometric equilibrium module, so that the reaction stoichiometry is specified. Such a modeling choice is required to exclude the steam reforming reaction from chemical equilibrium computations. In fact, such a reaction is kinetically hindered by the low temperature in the shift reactor.

The PSA is simulated through a black-box phenomenological model that relies on the PSA experimental efficiency curve as a function of its pressure, ranging from about 76% at 8 bar and 85% at 20 bar.

The heat exchangers HE-1, HE-2, HE-3, and HE-5 require an accurate modeling of the off-design operations, since mass flow rates of both hot and cold streams are determined by the desired H_2 production rate. Under design conditions all the temperatures are fixed and the thermal resistance (R^*) can be determined as [17]:

$$R^* = Q/\Delta T_{ml} \tag{1}$$

being Q the thermal power and ΔT_{ml} the logarithmic mean temperature difference. The off-design thermal resistance R is estimated as

$$R = R^*(\dot{m}/\dot{m}^*)^{0.8} \tag{2}$$

The ratio between the actual and the design mass flow rates, $\dot{m}/\dot{m}^*$, is estimated with reference to both the cold and the hot streams, having fixed the steam to NG ratio. For the other heat exchangers the cooling flow can be adjusted to meet the desired outlet temperature for the reacting gasses. Thus, off-design modeling is not required.

The FC model, schematically depicted in Fig. 1(b), features the PEM stack, the air processing unit, that represents the control system of the fuel cell system and determines the air flow based on the FC working conditions, an air compressor, and two cooling circuits that allow recovering the thermal energy from the FC for cogeneration. The performance of the FC is calculated from the experimental data provided by NuCellSys on the automotive FC system and reported in Fig. 2 in non-dimensional form. The model takes the hydrogen mass flow rate as input, and returns, as output, the mass flow rate of the required air flow, the exhaust mass flow rate and composition, the FC net electrical power, the cogenerated thermal power, and purge and/or leakages mass flow rate and composition.

Heat is co-generated from different sources: the high temperature cooling circuit, the low temperature cooling circuit, and the exhaust stream. The low temperature cooling circuit is designed to drain from the stack 2 kW of thermal power in any working conditions. The thermal power retrieved from the high temperature cooling circuit varies as a function of the FC load and is calculated as $Q_{HT} = \dot{m}_{HT}(h_{HT}^{out} - h_{HT}^{in})$, being $\dot{m}_{HT}$ the mass flow rate of the coolant, and h_{HT}^{in} and h_{HT}^{out} are its enthalpies at the inlet and at the outlet of the stack, respectively. Similarly, the thermal energy retrieved from the exhaust stream is $Q_{exh} = \dot{m}_{exh}(h_{exh}^{in} - h_{exh}^{out})$, where $\dot{m}_{exh}$ is the exhaust mass flow and h_{exh}^{in} and h_{exh}^{out} are its enthalpies at the inlet and outlet of the heat exchanger. Enthalpies are calculated from temperature, pressure, and composition of each stream according to the Peng-Robinson equation of state.

Several fluid machineries are present to provide the needed pressure level (see Fig. 1): a NG compressor; two air compressors (one for the burner and one for the FC); four circulation pumps (two for the reformer and two for the FC). The mechanical power required by each of these fluid machineries is calculated as

$$W_{aux} = \eta(h^{out} - h^{in}) \quad (3)$$

where the enthalpies are estimated accounting for the real fluid behavior through the Peng-Robinson equation of state, and the efficiency (η) is retrieved from the Aspen Plus turbo-machinery database as a function of the mass flow rate and of the head.

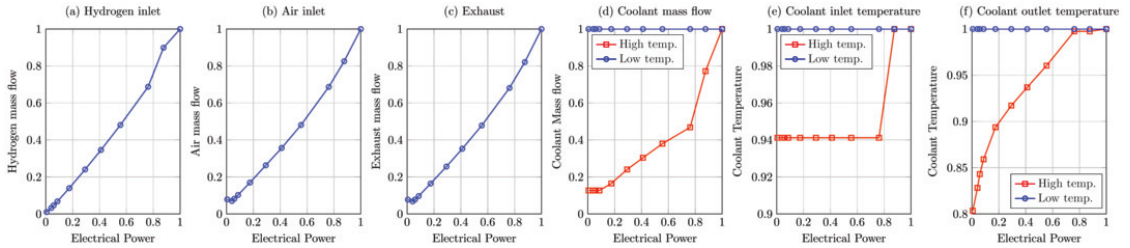

Fig. 2 - Experimental performances of the automotive fuel cells system manufactured by NuCellSys. All data are in non-dimensional form.

4. Results and discussion

The performance of the CHP plant is dissected varying the NG mass flow rate and the pressure, considering the NG flow rate higher than 50% of the nominal value and that the pressure can be varied in the range 8 bar - 12 bar. Fig. 3 reports the mass and energy fluxes of the baseline plant configuration (see Fig. 1). Specifically, Fig. 3(a) compares the hydrogen mass flow rate to the NG input and demonstrates that the reformer efficiency is not significantly influenced by the set point. In fact, $\dot{m}_{H_2}$ increases linearly by increasing the NG mass flow. The rate of variation of the electrical power with increasing NG flow rates is less than linear, thus indicating that η_{gob} is maximized at low loads.

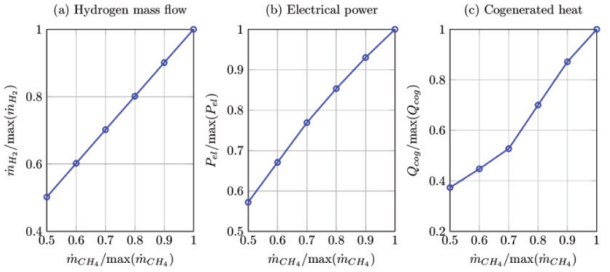

Fig. 3 - Energy and mass fluxes of the plant as function of the natural gas pressure for a reformer pressure of 12 bar: (a) Hydrogen produced by the reformer; (b) Net electrical power of the FC; and (c) Cogenerated heat. Results are displayed in non-dimensional form.

Table 1. Maximum efficiency for different natural gas pressures for the baseline and the modified CHP plant.

	Baseline		Modified	
	$\max(\eta_{glob})$	$\max(\eta_{total})$	$\max(\eta_{glob})$	$\max(\eta_{total})$
NG pressure 1 bar	37.8%	81.3%	40.0%	77.7%
NG pressure 12 bar	39.1%	82.5%	41.2%	79.0%

The maximum efficiency of the CHP plant is reported in Table 1 for different NG pressure levels. As expected, the efficiency of the FC is maximized at the minimum load (see Fig. 4(a)). The electrical efficiency of the power plant ranges from 37.8% to 39.1 %, while the total efficiency varies between 81.3% and 82.5%: They are represented in Fig. 4(b) for two limiting cases: with the NG distributed at high pressure (>11 bar) and at 1 bar. By increasing the NG flow

rate, η_g is first reduced, and for flow rates larger than 70% of the maximum, is increased up to its maximum. For NG flow rates <70% the electrical power reduction is more relevant with respect to the thermal power raise. Conversely, for $\dot{m}_{CH_4}/\max(\dot{m}_{CH_4}) > 0.7$, a higher increase of the thermal power (see Fig. 3(c)) contributes to the increase of η_t.

Fig. 4(b) and 4(c) show that the electrical consumption of the auxiliaries has a significant impact on the CHP plant performances. In fact, at 12 bar, the total consumption of the auxiliaries is about 4% of the overall electrical power. The pressure of the syngas influences both the consumption of the auxiliaries and the efficiency of the PSA (see Fig. 2). These drivers have opposite effects on the plant efficiency. The overall effect of the reforming pressure on the CHP plant efficiency is depicted in Fig. 5, for the maximum and the minimum NG mass flow rates. Both η_g and η_t are increased by increasing the NG pressure, regardless to $\dot{m}_{CH_4}$. Coherently with the results reported in Fig. 4, in the whole range of operating pressure, the electrical efficiency is maximized at the minimum power. On the contrary, the total efficiency is maximized at maximum power irrespective of the operating pressure.

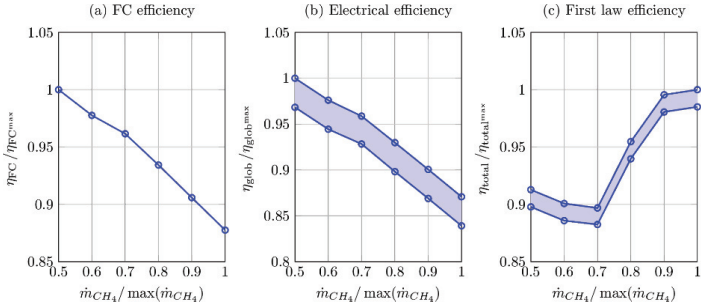

Fig. 4 - Efficiency of the CHP plant for a reformer pressure of 12 bar. The blue band between identifies the performances with and without including the work for NG compression. Results are displayed in non-dimensional form.

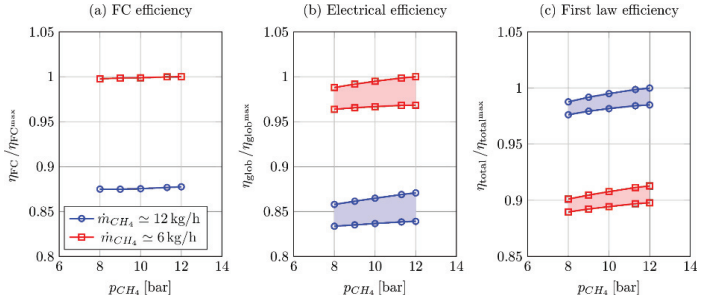

Fig. 5 - Efficiency of the CHP plant as a function of the NG pressure at minimum (red line) and maximum (blue line) flow rate. The blue and red bands identify the range of performances with and without including the work for NG compression. Results are displayed in non-dimensional form.

We note that η_{FC} has a significant influence on the CHP system efficiency and that it is maximized at the minimum load. Thereafter, we hypothesize to improve the baseline plant efficiency by using two fuel cells in parallel. Being the total H_2 flow rate identical with respect to the baseline plant, in the improved version each FC is operated at a lower load. In this configuration, the electrical efficiency is improved thanks to the favorable part load behavior of the fuel cells, as evidenced in Fig. 6(b) and in Table 1, where the efficiencies of the baseline and the modified CHP plants are compared. We observe that the data reported in Fig. 8 are normalized with respect to the maximum efficiencies of the baseline plant, allowing for an immediate comparison between the baseline and the modified configurations. Specifically, Fig. 6 shows that η_g is increased of about 5% with respect to the baseline configuration, exceeding 40%. The total efficiency is reduced with respect to the baseline plant (see Fig. 6(c)), due to the reduced load of the FC. We also note that, differently from the baseline configuration, the total efficiency is now reduced by increasing the load, being the set-point of the FCs always lower than 70%. The effect of p_{CH_4} on the CHP plant efficiency is displayed in Fig. 7. The electrical efficiency is moderately increased by increasing the NG pressure. The total efficiency still increases by increasing p_{CH_4}, but, differently from the baseline plant η_{total} is higher for a larger $\dot{m}_{CH_4}$.

5. Conclusions

We numerically analyzed the performances of an innovative CHP plant based on an automotive derivative PEM FC. The energy system includes a fuel processor based on auto-thermal reforming, water gas shift reaction and PSA that convert the NG into pure H_2. Results show that the main driver influencing the plant efficiency are the plant load and the NG delivery pressure. For the baseline plant, the electrical efficiency is maximized at part load, while the total efficiency is maximized at full load. Splitting the hydrogen flow into two identical FCs improves the overall performances, thanks to the favorable part load behavior of the PEM.

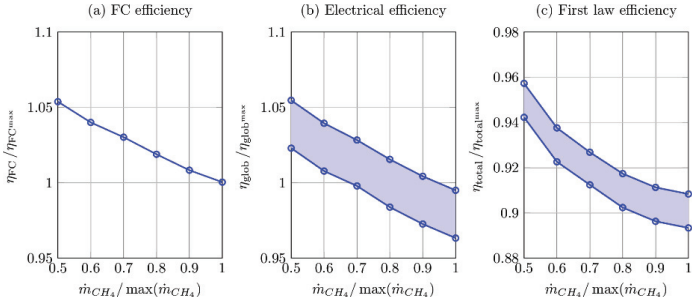

Fig. 6 - Efficiencies of the modified CHP plant. Results normalized with respect to the baseline plant.

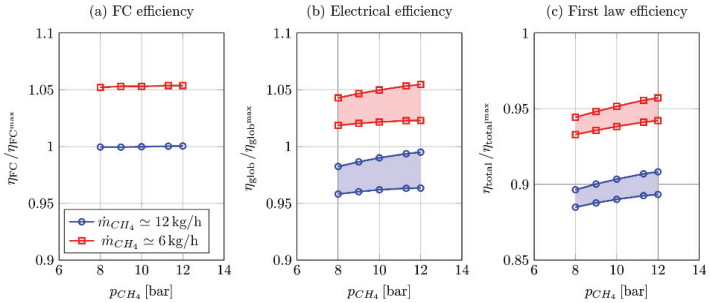

Fig. 7 - Efficiencies of the modified CHP plant. Results normalized with respect to the baseline plant.

Acknowledgements

This project has received funding from the Fuel Cells and Hydrogen Joint Undertaking under grant agreement No 671396. This Joint Undertaking receives support from the European Union's Horizon 2020 research and innovation programme and United Kingdom, Germany, Greece, Croatia, Italy, Switzerland, Norway. Swiss partners are funded by the State Secretariat for Education, Research and Innovation of the Swiss Confederation.

References

[1] International Energy Agency, *IEA advanced fuel cells implementing agreement and annual report*, 2010.
[2] Guzy, C. PEM fuel cells for distributed generation, in *Washington fuel cell summit*, 2012.
[3] FCH JU, http://www.fch-ju.eu/page/documents.
[4] Fuel cell today, *2010 Survey of Corea*, 2011.
[5] Fuel cell today, *The industry review 2013*, 2013.
[6] G. Saur, Stationary Fuel Cell Evaluation, in *DOE Annual Merit Review National Renewable Energy Laboratory*, 2014.
[7] Staffell, I., and Green, R. (2013). *International Journal of hydrogen energy*, 38(2), 1088-1102.
[8] Gigliucci, G., Petruzzi, L., Cerelli, E., Garzisi, A., & La Mendola, A. (2004) *Journal of Power Sources*, 131(1), 62-68.
[9] Tang, Y., Yuan, W., Pan, M., Li, Z., Chen, G., & Li, Y. (2010). *Applied Energy*, 87(4), 1410-1417.
[10] Campanari, S., Valenti, G., Macchi, E., Lozza, G., & Ravidà, N. (2014). *Applied Thermal Engineering*, 71(2), 714-720.
[11] Cozzolino, R., Cicconardi, S. P., Galloni, E., Minutillo, M., & Perna, A. (2011). *International Journal of Hydrogen Energy*, 36(13), 8030-8037.
[12] Barelli, L., Bidini, G., Gallorini, F., and Ottaviano, A. (2012). *Applied Energy*, 91(1), 13-28.
[13] Cappa, F., Facci, A. L., and Ubertini, S. (2015). *Energy*, *90*, 1229-1238.
[14] European Patent 94600005.6/13.07.94. U.S.A. Patent No. 6, 605 376 Aug. 12 .2003
[15] Piga, A., and Verykios, X. E. (2000). *Catalysis today*, 60(1), 63-71.
[16] Aspen Tech, Aspen Plus Unit Operation Models Reference Manual.
[17] Kreith, F., Manglik, R. M., and Bohn, M. S. (2012). *Principles of heat transfer*. Cengage learning.